International Journal of Design & Nature and Ecodynamics
Vol. 20, No. 12, December, 2025, pp. 2821-2829
Journal homepage: http://iieta.org/journals/ijdne

Waste to a Value-Added Material: Production of Biochar from Young Coconut Waste

Khairul Anwar[1], Mahidin[1,2*], Ichwana Ramli[3], Muhammad Faisal[1,2], Hera Desvita[4], Yeni R. Wulandari[5], Muhammad Z. Ramli[6]

[1] Graduate School of Engineering, Universitas Syiah Kuala, Banda Aceh 23111, Indonesia
[2] Department of Chemical Engineering, Faculty of Engineering, Universitas Syiah Kuala, Banda Aceh 23111, Indonesia
[3] Department of Agriculture Engineering, Faculty of Agriculture, Universitas Syiah Kuala, Banda Aceh 23111, Indonesia
[4] Research Center for Food Technology and Processing, National Research and Innovation Agency (BRIN), Yogyakarta 55861, Indonesia
[5] Department of Industrial Chemical Engineering Technology, Politeknik Negeri Lampung, Bandar Lampung 35144, Indonesia
[6] Faculty of Chemical Engineering, Universiti Teknologi MARA, Permatang Pauh 13500, Malaysia

Corresponding Author Email: mahidin@usk.ac.id

https://doi.org/10.18280/ijdne.201208

Received: 30 September 2025
Revised: 16 December 2025
Accepted: 24 December 2025
Available online: 31 December 2025

Keywords:
functional groups, heating rate, pyrolysis, specific surface area, thermal decomposition, young coconut waste

ABSTRACT

Young coconut waste (YCW) holds considerable potential as a lignocellulosic biomass feedstock for sustainable biochar production. Indonesia has substantial potential for utilizing young coconut biomass waste, yet its use to date remains largely confined to small-scale and specific applications. This study aims to investigate the thermal decomposition behavior, functional group transformations, surface characteristics, and adsorption potential of biochar derived from YCW through pyrolysis at 300, 350, and 400°C, temperatures selected to capture the transition between initial devolatilization and the onset of aromatic structure formation. TG–DTG analysis was conducted to assess thermal stability within the temperature range of 25–700°C at heating rates of 10, 15, and 20°C/min, while FTIR spectroscopy and nitrogen adsorption–desorption isotherms were employed to characterize chemical functional groups and SBET, respectively. TG–DTG curves showed that the heating rate significantly affected the thermal stability of YCW, with a heating rate of 10°C/min resulting in more controlled decomposition and a higher biochar yield. FTIR spectroscopy analysis indicated the degradation of C=O, –OH, and C–H groups, along with the formation of aromatic C=C bonds, particularly at 350°C. Biochar produced at 350°C exhibited the most favorable pore development and surface chemistry. The highest BET surface area was recorded for YCW350 (1.298 m²/g), followed by YCW300 (1.266 m²/g), with a substantial decrease observed for YCW400 (0.127 m²/g) due to pore collapse. These findings provide an initial physicochemical characterization of YCW biochar, with enhanced thermal stability and chemical reactivity, offering potential applications in energy systems and agricultural waste utilization.

1. INTRODUCTION

Indonesia is a tropical country that generates a considerable amount of waste from the agricultural and forestry sectors. One of the commonly encountered types of waste is young coconut waste (YCW). To date, YCW is generally disposed of directly into the environment without undergoing any treatment, which can potentially cause pollution and have adverse impacts on environmental quality. After being examined, YCW waste has the potential to be utilized as a raw material for promising carbon materials, particularly biochar derived from biomass. The availability of YCW, which consists of fibers and shells, is very abundant but has not been utilized optimally. Globally, the highest coconut production is in tropical regions such as Indonesia, India, the Philippines, Sri Lanka, Malaysia, Thailand, Papua New Guinea, and Fiji [1]. In 2023, Indonesia ranked first as the highest coconut-producing country in the world, surpassing the Philippines with a total production of 17.97 million metric tons [2]. The high volume of production significantly contributes to the accumulation of solid waste [1]. As a result, the organic waste generated from these activities has an impact on the proportion of organic waste, which has reached 50-60% of the total urban solid waste and poses serious environmental challenges due to its decomposition process, which produces greenhouse gases and leachate [3]. One of the methods that is starting to be developed for processing biomass into biochar is through the pyrolysis method.

The pyrolysis process is very helpful in addressing this issue by involving the heating of biomass under inert conditions to decompose complex organic compounds into simpler products such as charcoal, pyrolysis gas, and bio-oil. In the development of carbon materials, one of the main parameters that needs to be controlled is the temperature of pyrolysis, as

it greatly affects the chemical structure and porosity characteristics of the resulting material [4]. As the pyrolysis temperature increases from 300–600°C, there is an enhancement in the devolatilization and carbon restructuring processes, which can result in a larger specific surface area and a more uniform pore distribution [5]. Previous studies reported that biochar derived from the branch and leaf parts of Pond cypress (*Taxodium ascendens*) pyrolyzed at 350, 450, 650, and 750°C for 30, 60, and 120 minutes showed that increasing pyrolysis temperature promoted greater release of volatile compounds, thereby enhancing porosity and specific surface area, with the highest SSA of 744 $m^2 g^{-1}$ obtained at 750°C for 60 minutes, while a more stable carbon structure was achieved at 650°C for 30 minutes [6].

This phenomenon is closely related to the thermal degradation mechanisms of the main components of biomass, namely cellulose, hemicellulose, and lignin. Cellulose begins to degrade at a temperature around 300°C, producing volatile compounds in the form of gas and bio-oils, as well as charcoal as a byproduct [7]. Hemicellulose has a lower degradation point, between 200–300°C. It significantly contributes to the formation of volatile compounds during the pyrolysis process [8]. Meanwhile, lignin is the most thermally stable component, degrading at temperatures above 400°C and producing various complex aromatic compounds [9]. Besides the pyrolysis temperature, several other parameters influence the quality and characteristics of the produced biochar, including the heating rate, residence time in the pyrolysis reactor, biomass feedstock characteristics, and the pyrolysis atmosphere. A higher heating rate can accelerate the devolatilization process and increase the reactivity of biochar [10]. A longer residence time in the reactor facilitates more complete breakdown of volatile chemicals, which in turn boosts the structural quality and carbonization degree of the resulting biochar [11]. Because lignin breaks down more slowly and aids in the development of condensed aromatic compounds, prior research has also demonstrated that biomass with a high lignin concentration tends to produce biochar with greater thermal stability and a larger surface area [12]. Furthermore, by changing the formation of pore networks and the preservation or removal of surface functional groups, the surrounding pyrolysis atmosphere—whether inert or reactive—can further affect these results [13]. All of these results demonstrate how residence duration, feedstock content, and processing environment interact to influence the properties of biochar.

Building on these ideas, characterizing biochar becomes crucial to comprehending for understanding how production conditions affect its structure. In particular, FTIR analysis makes it possible to identify functional-group transformations both before and after pyrolysis, providing information about the organic component breakdown routes and the reorganization of carbon frameworks under various processing temperatures and atmospheres [14]. FTIR spectrum allows the detection of various functional groups such as hydroxyl (–OH), carboxyl (–COOH), esters (–O–CO–), amine ($–NH_2$), and carbon-carbon double bonds (C=C), all of which contribute to the adsorption capacity of biochar in energy storage and waste treatment applications [15]. In addition, the initial thermal characteristics of raw materials can be evaluated using TGA testing to assess mass changes due to thermal degradation [16], while thermogravimetric-derivative thermogravimetric (TG-DTG) analysis is widely applied to assess thermal stability, identify decomposition stages and their corresponding degradation rate peaks, and estimate residual yield at the end of the process stage. Meanwhile, the specific surface area is calculated using the BET method to measure the specific surface area and pore size distribution, which is an important parameter in assessing the feasibility of biochar as a material for gas storage or adsorption of certain substances [17]. This characterization of specific surface area and pore structure is particularly relevant when linked to the thermal behavior of biochar, as demonstrated in previous studies on YCW biomass pyrolysis.

Based on these findings and the growing interest in sustainable biomass conversion, understanding the pyrolysis characteristics of YCW is important for assessing its suitability as a feedstock for producing high-quality biochar. Accordingly, this study investigates the effect of pyrolysis temperature (300, 350, and 400°C) on the conversion of YCW into biochar. Specifically, the temperature-dependent changes in thermal behavior at different heating rates (10, 15, and 20°C/min), chemical structure, and textural properties associated with the BET specific surface area (S_{BET}) were evaluated. The results are expected to provide a robust scientific basis for elucidating the relationship between pyrolysis conditions and the properties of YCW-derived biochar, thereby supporting its further development and utilization as a porous carbon material for various applications, including energy-related uses.

2. METHODOLOGY

2.1 Materials and equipment

YCW was collected from local coconut drink vendors. The waste consisted primarily of husks and shells that remained after the extraction of coconut water. The YCW samples were converted into biochar using a pyrolysis device equipped with a heater, a temperature control system, and a Type-K thermocouple sensor, as shown in Figure 1. Additional equipment included an oven (Gemmy888 YCO-010), an analytical balance, a grinding machine, and a crucible. The characterization of the biochar's functional groups, thermal properties, and surface area and porosity was performed using a Fourier Transform Infrared Spectrometer (FTIR, Shimadzu IR Prestige 21), a thermogravimetric analyzer (TGA, SDT-Q600 TA Instruments), and a surface area and porosity analyzer (Micromeritics ASAP 2020).

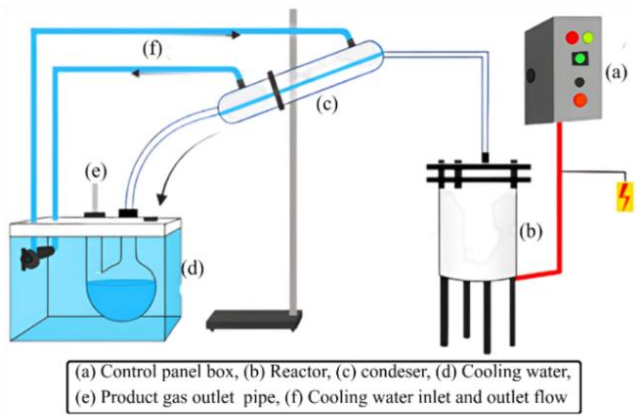

Figure 1. Schematic diagram of the biomass pyrolysis unit using a batch reactor [18]

2.2 Preparation of biochar

YCW, consisting of husk and young coconut shells, was cut into 5 × 5 cm pieces and sun-dried for approximately three days to reduce moisture content to 20%. The dried YCW biomass was weighed at 250 g and then pyrolyzed in a slow-pyrolysis reactor at 300, 350, and 400°C for 120 minutes, under limited oxygen to prevent combustion. After pyrolysis, the resulting biochar was ground and filtered through a 60-mesh sieve. The biochar samples were designated YCW300, YCW350, and YCW400 according to their respective pyrolysis temperatures.

2.3 Specific surface area (S_{BET})

Specific surface area analysis was conducted on the pyrolysis products obtained at treatment temperatures of 300, 350, and 400°C. This analysis was essential for evaluating the material's potential for energy storage or other adsorption-based applications. Before the analysis, the samples underwent a degassing process under vacuum conditions at 200°C for 120 minutes. This step aimed to remove water vapor or gases that may have been adsorbed onto the pore surfaces, thereby improving the accuracy of the results. Following degassing, the samples were exposed to nitrogen gas at a cryogenic temperature of -196°C. The nitrogen gas adhered to the pore surfaces of the sample at various partial pressures, which were then used to construct an adsorption isotherm curve. This curve describes the relationship between the amount of gas adsorbed and the relative pressure (P/P_0). It was subsequently used to calculate the specific surface area based on the BET equation Eq. (1).

$$\frac{1}{W\left(\frac{P_0}{P}-1\right)} = \frac{1}{W_m C} + \left(\frac{C-1}{W_m C}\right)\frac{P}{P_0} \quad (1)$$

where, W is the weight absorbed at relative pressure (P/P_0), W_m is the amount of nitrogen adsorbed to form a monolayer on the surface, P is the equilibrium adsorption pressure, P_0 is the saturation pressure of adsorption-desorption of the sample at the cooling immersion temperature, and C is the BET constant related to the adsorption energy.

3. RESULTS AND DISCUSSION

3.1 TG-DTG analysis

TG-DTG analysis provides insight into the thermal properties of YCW, showing the pattern of mass degradation and linear heating rate over time. Mass loss observations were made at three heating rates, namely 10, 15, and 20°C/min. The TG-DTG test results shown in Figure 2 indicate a gradual mass loss pattern, reflecting the thermal decomposition process of organic components in YCW biomass. Table 1 summarizes the thermal decomposition behavior of YCW biomass, which occurs in four distinct stages. The first stage (< 200°C) showed mass loss of 20.29%, 12.12%, and 10.00% at heating rates of 10, 15, and 20°C/min, respectively. The second stage (200–350°C) is the phase with the greatest mass loss, namely 49.72%, 44.30%, and 40.67% in sequence. In the third stage (350–500°C), mass loss was 13.39%, 13.03%, and 12.75%, while in the fourth stage (500-700°C), mass loss was lower, namely 11.17%, 10.43%, and 9.89% for each heating rate.

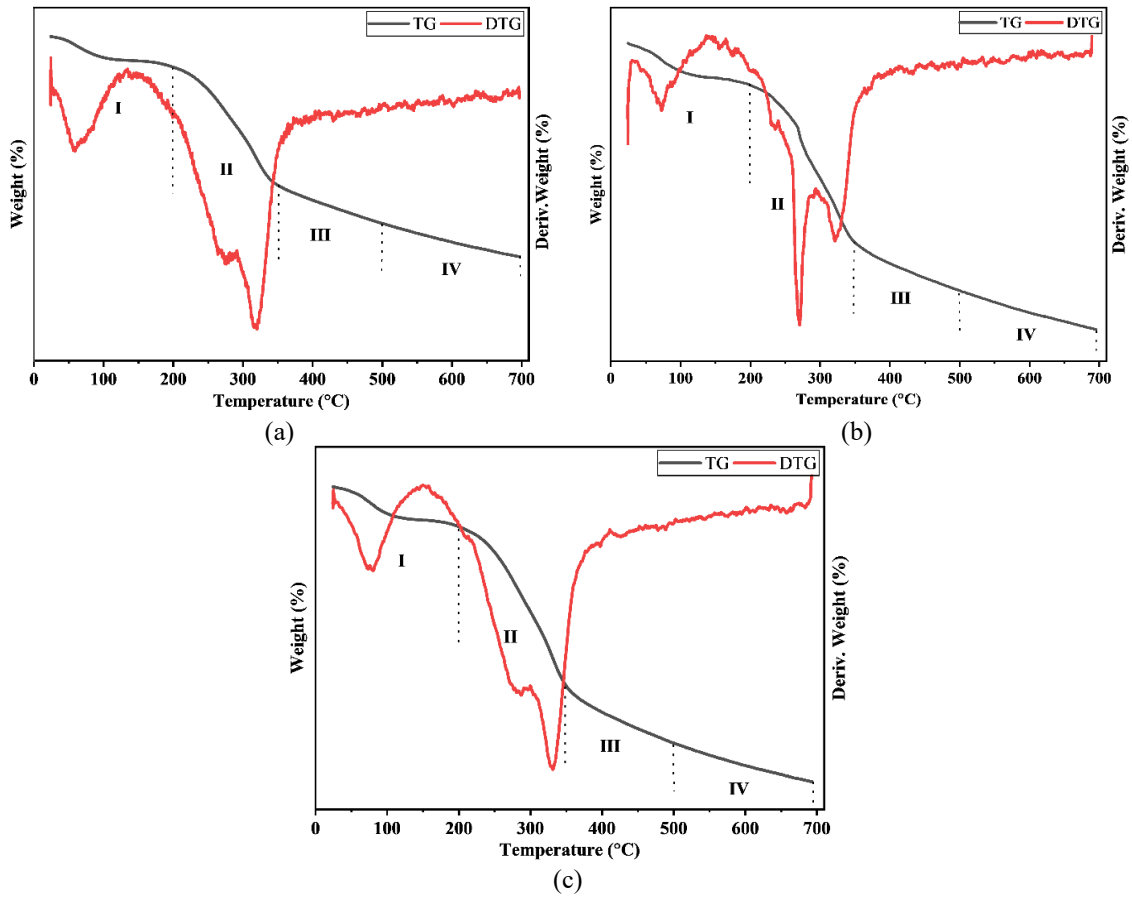

Figure 2. TG-DTG decomposition stages of YCW (a) Heating rate of 10°C/min; (b) Heating rate of 15°C/min; (c) Heating rate of 20°C/min

Table 1. Thermal decomposition stages of YCW biomass at different heating rates

Heating Rate (℃/min)	Temperature Range (℃) and Mass Loss (%)			
	(I) < 200	(II) 200-350	(III) 350-500	(IV) 500-700
10	20.29	49.72	13.39	11.17
15	12.12	44.30	13.03	10.43
20	10	40.67	12.75	9.89

Differences in heating rates affect the degradation rate and final pyrolysis yield, where higher heating rates generally result in lower biochar yields [19]. These results are consistent with previous findings, which report that YCW contains approximately 32% cellulose, 38% lignin, and 0.25% hemicellulose, with cellulose and lignin content ranging between 37.2% and 43.9%, depending on the maturity stage of the coconut [20]. Lignin, an amorphous polymer with complex cross-linking and no defined structure, undergoes degradation over the temperature range of 280–500°C. This range indicates high thermal stability because the rate of decomposition tends to decrease as the temperature increases [21].

The decrease in mass loss in the first stage is related to the evaporation of free and bound water [22], where the slow heating rate allows sufficient time for more complete water removal [23]. In the second stage, the decomposition of hemicellulose dominates, along with significant breakdown of cellulose [24], which is the most thermally reactive volatile component [5]. The third stage of lignin decomposition is slower and more stable, resulting in relatively constant mass loss. The fourth stage of decomposition slows down further, indicating the formation of stable biochar [25]. In addition to these stage-wise trends, the decrease in total mass loss with increasing heating rate also indicates that higher heating rates produce larger final solid fractions. This suggests that the thermal stability of biochar increases even in oxygen-rich atmospheric conditions [26]. Meanwhile, at a heating rate of 10°C/min, clearer decomposition peaks at each stage indicate a more defined and gradual pyrolysis process, which can provide an overview of the formation of a more uniform and controlled biochar structure, especially in relation to carbon material design for various applications, including the energy sector.

3.2 Functional groups analysis by FTIR

FTIR was used to identify the functional groups in YCW biochar produced at different pyrolysis temperatures. Based on the FTIR spectrum, changes in the chemical structure of biochar can be analyzed from the shift in wave numbers and specific peaks of functional groups. FTIR spectrum of biochar after the pyrolysis process at temperature variations of 300, 350, and 400°C, respectively denoted as YCW300, YCW350, and YCW400. The results of FTIR are presented in Figure 3.

Figure 3 shows the FTIR spectra of YCW biochar produced at pyrolysis temperatures of 300, 350, and 400°C. A broad absorption band around 3600 cm^{-1}, associated with hydroxyl (–OH) functional groups, is observed in all samples, with decreasing intensity as pyrolysis temperature increases. The aliphatic C–H stretching band at 3046 cm^{-1} and the CH_3 symmetric stretching band at 1432 cm^{-1} are also present, but their intensities progressively weaken at higher temperatures. A dominant absorption band at 2359 cm^{-1} is detected in all spectra. In addition, a band at 1615 cm^{-1} appears and becomes more pronounced with increasing pyrolysis temperature. The FTIR band at 1265 cm^{-1}, corresponding to C–O functional groups, is evident at lower temperatures and shows a reduction in intensity as the pyrolysis temperature increases.

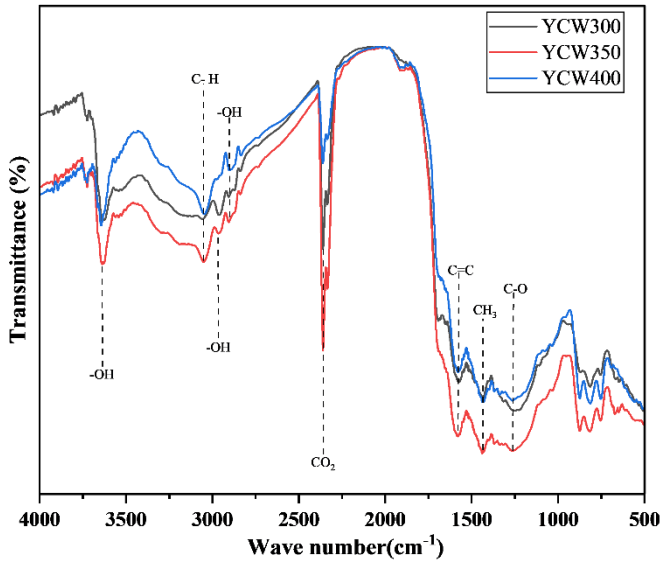

Figure 3. FTIR spectra of YCW-derived biochar obtained under various pyrolysis conditions

The decrease in intensity of the –OH band at ~3600 cm^{-1} with increasing pyrolysis temperature is associated with the reduction of hydroxyl functional groups in YCW biochar [27]. This behavior is attributed to the loss of hydrogen-bonded structures arising from inter- and intra-molecular stretching vibrations in polymeric compounds such as lignin and cellulose [28]. The weakening of aliphatic C–H stretching at 3046 cm^{-1} [29] and CH_3 symmetric stretching at 1432 cm^{-1} [30] with increasing temperature indicates the degradation of aliphatic hydrocarbons. These functional groups are primarily derived from cellulose and hemicellulose components in YCW [31], and their reduction reflects depolymerisation and volatilization of light organic fractions during pyrolysis.

The dominant absorption band at 2359 cm^{-1} corresponds to CO_2, consistent with previous reports indicating that the 2340–2360 cm^{-1} region represents the asymmetric stretching vibration (v_3) of CO_2 in the FTIR optical path [32]. The increased prominence of the absorption band at 1615 cm^{-1} is attributed to C=C stretching associated with pyrrole ring structures [33]. This trend suggests progressive aromatization and condensation reactions occurring at higher pyrolysis temperatures, which are characteristic of advanced stages of biochar formation. The FTIR band at 1265 cm^{-1} indicates the presence of C–O bonds from ether functional groups (R–O–R), consistent with reported FTIR characteristics for C–O stretching vibrations in the 1300–1210 cm^{-1} range [27, 34, 35]. The weakening of this band with increasing pyrolysis temperature reflects the decomposition of oxygen-containing functional groups [22] and indicates the transition of biochar toward a more stable, carbon-rich structure with reduced oxygen functionality [36].

The presence of hydroxyl groups (-OH) and (CO_2) in excess can disrupt the thermal stability of biochar as an energy source. However, as the pyrolysis temperature increases, the presence of these components in biochar can be reduced [37]. In addition, biochar with a high (-OH) content at 350°C shows a tendency to absorb moisture, which causes difficulties in ignition and reduces shelf life. However, hydroxyl groups (-

OH) can also enhance the reactivity of biochar, especially under limited air combustion conditions, as they can accelerate the initial oxidation reaction by releasing water vapor and volatile gases, thereby speeding up the ignition process [6].

The temperature of pyrolysis plays an important role in determining the functional groups and characteristics of the produced biochar. At low temperatures (200–300°C), biochar still retains oxygenation groups such as hydroxyl (-OH) and carbonyl (C=O), which increase its reactivity but reduce thermal stability. Previous research has shown that biochar produced at a temperature of 250°C retains a larger proportion of carboxyl (-COOH) and hydroxyl (-OH) oxygenated groups, which play a role in nutrient retention in the soil [38]. As the temperature increases to 300–400°C, there is decomposition of volatile compounds and carbon restructuring, leading to the formation of aromatic C=C bonds and a decrease in oxygen content. The transformation is triggered by the dehydration and depolymerization processes, which gradually remove the oxygenated groups and allow the formation of more stable carbon structures [39]. Aromatic carbon structures are formed at higher temperature ranges with thermal stability and long-term carbon resistance [40]. Therefore, controlling the pyrolysis temperature becomes the main factor in determining the optimal properties of biochar, depending on its application, whether as a solid fuel, energy storage, or gas adsorption in sustainable energy systems [41].

3.3 Adsorption-desorption isotherms

Figure 4 shows the nitrogen adsorption-desorption isotherm of biochar samples produced from YCW at pyrolysis temperatures of 300°C, 350°C, and 400°C. The pyrolysis temperature has a significant influence on the adsorption and desorption capacity as well as the surface characteristics of the biochar. The adsorption capacity increases with rising temperature until it reaches a maximum at 350°C. This is evidenced by the fact that higher temperatures lead to increased surface roughness and the formation of macropores, thereby contributing to improved adsorption efficiency [4]. Similar research was also reported by Naghipour et al. [42], where the increase in carbonization temperature improved the surface area and adsorption efficiency of activated carbon made from various precursors, including biomass waste. The optimum adsorption performance was shown in YCW350 biochar, possibly due to the balance between pore structure development and the presence of preserved active functional groups [43].

However, at a temperature of 400°C, there is a decrease in adsorption capacity. This is likely due to the degradation of active compounds and changes in the surface characteristics of biochar because of high-temperature treatment [44, 45]. A study [46] highlights that excessive increase in carbonization temperature can lead to surface restructuring that reduces adsorption capacity, even though porosity is increased. Other possible indications due to the loss of active chemical groups remaining on the surface of biochar due to increased temperature [47], and the pores of biochar can become clogged by excessive ash deposits [48]. The results indicate that the optimal pyrolysis temperature is not linear, but rather must be adjusted according to the material properties of YCW. It can be concluded that there is an optimal limit to the pyrolysis temperature depending on the raw material used, where further increases in temperature can lead to the degradation of pore structure and reduce adsorption capacity. Thus, the observed FTIR spectrum results can also be related to the elemental composition and adsorption properties, with biochar that has prominent C=O and O–H groups potentially showing higher reactivity in soil amendment applications, while biochar with higher aromaticity tends to offer better stability and greater potential in carbon sequestration [31].

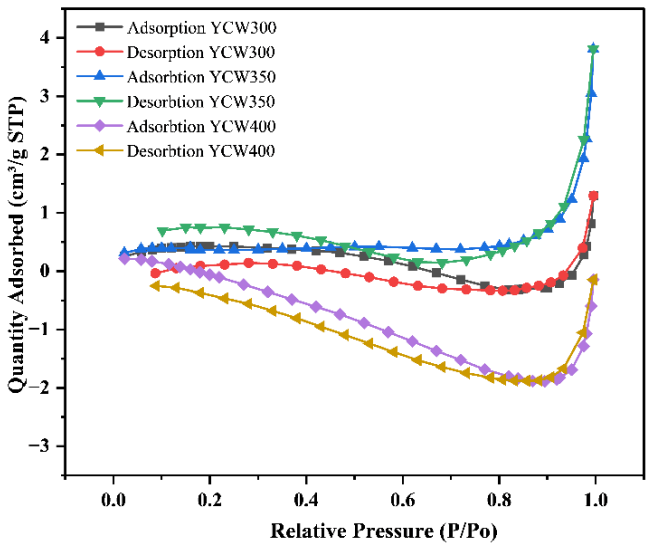

Figure 4. N_2 adsorption-desorption isotherms of YCW biochar

3.4 S_{BET} analysis of biochar

In Figure 5, the linear plot results from the Brunauer–Emmett–Teller model are used to determine the specific surface area of the biochar produced from YCW at YCW300, YCW350, and YCW400 pyrolysis temperatures. The analysis was conducted within the relative pressure range P/P_0 between 0.05 and 0.30 following the standard [49]. The results show significant differences in modeling quality and surface area estimates. For YCW300, a slope value of 3.497 and an intercept of –0.060 were obtained, with a coefficient of determination (R^2) of 0.96. Meanwhile, YCW350 had a slightly higher slope of around 3.943 and an intercept of (–0.089), with an R^2 of 0.983. Subsequently, YCW400 showed an increase in slope to 35.919, an intercept of (–1.725), and an R^2 value of 0.575.

To strengthen the interpretation of the results, the suitability of the linear model for the P/P_0 range used was further assessed using the R^2 value and the intercept characteristics for each sample. The low R^2 value in YCW400 indicates that the linear model is less capable of representing the data trend in the P/P_0 range used in the calculation. The negative intercept value indicates an increased adsorbate–adsorbent interaction within ultramicropores, arising from overlapping adsorption potentials generated by the pore walls [50]. Thus, the data points in the linear region of the BET plot are inadequate or unrepresentative, research [50, 51] and previous research [52] stated that some structures have BET areas that significantly exceed the actual monolayer area, but gas adsorption beyond the monolayer is still counted as part of the monolayer, which can create obstacles in the accurate application of the BET model.

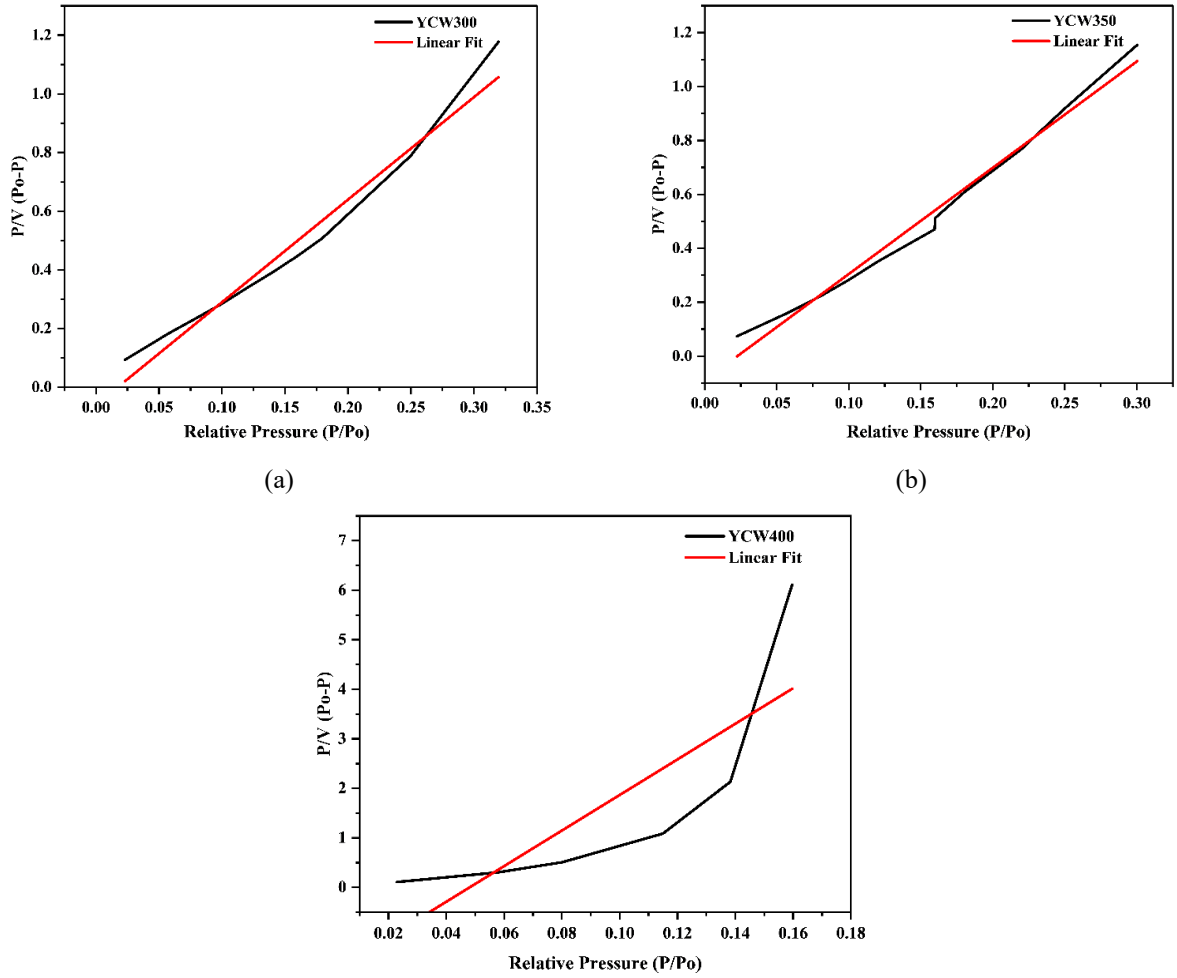

Figure 5. Linear BET fitting plots for YCW biochar (a) YCW300; (b) YCW350, (c) YCW400

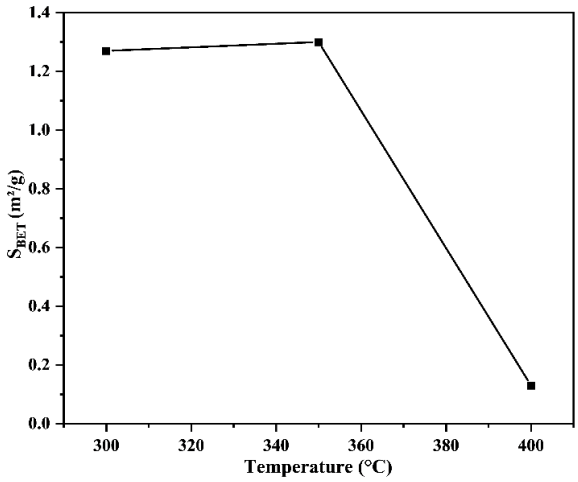

Figure 6. S_{BET} of biochar produced at 300, 350, and 400°C

The monolayer volume (W_m) is calculated using the equation that takes the reciprocal sum of the slope and intercept derived from the BET isotherm curve, which represents the amount of adsorbate gas that forms a monolayer on the solid surface. Furthermore, the S_{BET} is determined from the W_m value by converting it using the cross-sectional area of one adsorbate molecule on N_2 = 0.162 nm² and the Avogadro constant (-6.022 × 10^{23} mol^{-1}), thus resulting in the S_{BET} value in m²/g, which describes the total active surface area of the material available for adsorption. As shown in Figure 6, biochar YCW350 exhibits the highest S_{BET} (1.298 m²/g), followed by YCW300 (1.266 m²/g), and YCW400 with a markedly lower value of 0.127 m²/g. The linear slope for the YCW350 sample is greater than that of YCW300 and YCW400. Therefore, the highest S_{BET} value is found in YCW350, which is influenced by the differences in the intercept and constant values obtained during the calculation.

The S_{BET} of the YCW400 sample treatment decreased significantly compared to the YCW350 and YCW400 temperature treatments. This may occur because the very fast nitrogen adsorption at low pressure causes difficulties in the linear BET modeling, so that the total specific surface area is estimated inaccurately [53]. Previous research supports YCW400 on the limitations of the BET method in accessing narrow micropores and making it difficult to penetrate very small pore structures [54]. The basic assumption in the BET model becomes an issue when applied to biochar microporous materials, which generally have complex structures with high porosity and heterogeneous surfaces [53]. The model is designed to calculate S_{BET} but does not consider the pore volume filling mechanism that dominates in microporous structures [55]. Although the BET method provides a reliable comparative approach, a comprehensive understanding of biochar pore texture requires the integration of various characterization techniques.

4. CONCLUSIONS

This study shows that YCW undergoes a four-stage thermal degradation process, with a slower lignin-dominated breakdown above 500℃, following significant devolatilization at 200–350℃. Compared to heating rates of 15 and 20℃/min, a heating rate of 10℃/min showed clearer decomposition peak resolution, resulting in more stable biochar residue. The combined FTIR and nitrogen-sorption results show that while moderate temperatures (about 350℃) preserve important surface functionalities (–OH, C=O, –COOH) that improve reactivity and nutrient retention, higher temperatures cause a transition from oxygen-rich functional groups to more aromatic, thermally stable carbon structures. Depending on the required balance between usefulness and stability, these characteristics indicate that biochar from YCW has strong potential for various applications, including as a soil ameliorant, adsorbent, and carbon feedstock for energy applications. However, this study still has several limitations, mainly because the pyrolysis process was conducted on a laboratory scale and the variation in operating parameters examined was still limited to a specific temperature range and heating rate. More broadly, this study enriches our understanding of the conversion of tropical lignocellulosic biomass and reinforces the potential of YCW as a sustainable raw material. Further research is recommended by applying more sophisticated characterization techniques and by performing performance testing under real field conditions in accordance with the target application.

ACKNOWLEDGMENT

The author wishes to convey his utmost gratitude and appreciation to the Directorate General of Higher Education, Science and Technology, for funding this research under contract number: 162 /UN11.L1/ PG. D1.03/SPK/DPPM/2025, dated June 4, 2025. This financial support made it possible to carry out the study through to its completion and subsequent publication.

The authors gratefully acknowledge the Laboratory of the Chemical Engineering Department, Faculty of Engineering, UiTM Penang Island, and Syiah Kuala University for the facilities provided.

REFERENCES

[1] James, A., Yadav, D. (2021). Valorization of coconut waste for facile treatment of contaminated water: A comprehensive review (2010-2021). Environmental Technology & Innovation, 24: 102075. https://doi.org/10.1016/j.eti.2021.102075.

[2] Statista Research Department. (2025). Global leading producers of coconuts 2023. https://www.statista.com/statistics/1040499/world-coconut-production-by-leading-producers/.

[3] Pour, F.H., Makkawi, Y.T. (2021). A review of post-consumption food waste management and its potentials for biofuel production. Energy Reports, 7: 7759-7784. https://doi.org/10.1016/j.egyr.2021.10.119

[4] Chen, Y., Fan, C., Li, X., Ren, J., Zhang, G., Xie, H., Zhou, G. (2023). Preparation of carbon black-based porous carbon adsorbents and study of toluene adsorption properties. Journal of Chemical Technology & Biotechnology, 98(1): 117-128. https://doi.org/10.1002/jctb.7220

[5] Patra, B.R., Nanda, S., Dalai, A.K., Meda, V. (2021). Slow pyrolysis of agro-food wastes and physicochemical characterization of biofuel products. Chemosphere, 285: 131431. https://doi.org/10.1016/j.chemosphere.2021.131431

[6] Zhang, S., Hu, H., Jia, X., Wang, X., Chen, J., Cheng, C., Zhu, L. (2022). How biochar derived from pond cypress (Taxodium ascendens) evolved with pyrolysis temperature and time and their end efficacy evaluation. International Journal of Environmental Research and Public Health, 19(18): 11205. https://doi.org/10.3390/ijerph191811205

[7] Wang, K., Kim, K.H., Brown, R.C. (2014). Catalytic pyrolysis of individual components of lignocellulosic biomass. Green Chemistry, 16(2): 727-735. https://doi.org/10.1039/c3gc41288a

[8] Madhu, P., Vidhya, L., Vinodha, S., Wilson, S., Sekar, S., Patil, P.P., Prabhakar, S. (2022). Co-pyrolysis of hardwood combined with industrial pressed oil cake and agricultural residues for enhanced bio-oil production. Journal of Chemistry, 2022(1): 9884766. https://doi.org/10.1155/2022/9884766

[9] Mahmood, H., Ramzan, N., Shakeel, A., Moniruzzaman, M., Iqbal, T., Kazmi, M.A., Sulaiman, M. (2019). Kinetic modeling and optimization of parameters for biomass pyrolysis: A comparison of different lignocellulosic biomass. Energy Sources, Part A: Recovery, Utilization, and Environmental Effects, 41(14): 1690-1700. https://doi.org/10.1080/15567036.2018.1549144

[10] Czerski, G., Zubek, K., Grzywacz, P., Porada, S. (2017). Effect of char preparation conditions on gasification in a carbon dioxide atmosphere. Energy & Fuels, 31(1): 815-823. https://doi.org/10.1021/acs.energyfuels.6b02139

[11] Greco, G., Di Stasi, C., Rego, F., González, B., Manyà, J.J. (2020). Effects of slow-pyrolysis conditions on the products yields and properties and on exergy efficiency: A comprehensive assessment for wheat straw. Applied Energy, 279: 115842. https://doi.org/10.1016/j.apenergy.2020.115842

[12] Osman, A.I., Abdelkader, A., Johnston, C.R., Morgan, K., Rooney, D.W. (2017). Thermal investigation and kinetic modeling of lignocellulosic biomass combustion for energy production and other applications. Industrial & Engineering Chemistry Research, 56(42): 12119-12130. https://doi.org/10.1021/acs.iecr.7b03478

[13] Dong, Q., Zhang, S., Wu, B., Pi, M., Xiong, Y., Zhang, H. (2019). Co-pyrolysis of sewage sludge and rice straw: Thermal behavior and char characteristic evaluations. Energy & Fuels, 34(1): 607-615. https://doi.org/10.1021/acs.energyfuels.9b03800

[14] Janu, R., Mrlik, V., Ribitsch, D., Hofman, J., Sedláček, P., Bielská, L., Soja, G. (2021). Biochar surface functional groups as affected by biomass feedstock, biochar composition and pyrolysis temperature. Carbon Resources Conversion, 4: 36-46. https://doi.org/10.1016/j.crcon.2021.01.003

[15] Yaashikaa, P.R., Kumar, P.S., Varjani, S., Saravanan, A.J.B.R. (2020). A critical review on the biochar production techniques, characterization, stability and applications for circular bioeconomy. Biotechnology Reports, 28: e00570.

https://doi.org/10.1016/j.btre.2020.e00570
[16] Negara, D.N.K.P., Widiyarta, I.M., Karohika, I.M.G., Suriadi, I.G.A.K., Dwijana, I.G.K., Lokantara, I.P., Suarsana, I.K. (2023). Preparation and characterization of pelleted and powdered activated carbons derived from used brewed coffee. Trends in Sciences, 20(12): 7136-7136. https://doi.org/10.48048/tis.2024.7136
[17] Ajien, A., Idris, J., Md Sofwan, N., Husen, R., Seli, H. (2023). Coconut shell and husk biochar: A review of production and activation technology, economic, financial aspect and application. Waste Management & Research, 41(1): 37-51. https://doi.org/10.1177/0734242X221127167
[18] Wulandari, Y.R., Sukma, V.A., Supriadi, D., Mufti, A.A., Variyana, Y., Silmi, F.F., Wu, H.S. (2025). Kinetic investigation on thermal degradation of empty oil palm bunches pyrolysis. Periodica Polytechnica Chemical Engineering, 69(1): 67-77. https://doi.org/10.3311/PPch.38233
[19] Timilsina, M.S., Chaudhary, Y., Bhattarai, P., Uprety, B., Khatiwada, D. (2024). Optimizing pyrolysis and Co-Pyrolysis of plastic and biomass using Artificial Intelligence. Energy Conversion and Management: X, 24: 100783. https://doi.org/10.1016/j.ecmx.2024.100783
[20] Maulana, A., Prasetyo, T.B., Harianti, M., Lita, A.L. (2022). Effect of pyrolysis methods on characteristics of biochar from young coconut waste as ameliorant. IOP Conference Series: Earth and Environmental Science, 959(1): 012035. https://doi.org/10.1088/1755-1315/959/1/012035
[21] Gonzalez-Canche, N.G., Carrillo, J.G., Escobar-Morales, B., Salgado-Tránsito, I., Pacheco, N., Pech-Cohuo, S.C., Peña-Cruz, M.I. (2021). Physicochemical and optical characterization of citrus aurantium derived biochar for solar absorber applications. Materials, 14(16): 4756. https://doi.org/10.3390/ma14164756
[22] Zhao, S.X., Ta, N., Wang, X.D. (2017). Effect of temperature on the structural and physicochemical properties of biochar with apple tree branches as feedstock material. Energies, 10(9): 1293. https://doi.org/10.3390/en10091293
[23] Fraga, L.G., Silva, J., Teixeira, S., Soares, D., Ferreira, M., Teixeira, J. (2020). Influence of operating conditions on the thermal behavior and kinetics of pine wood particles using thermogravimetric analysis. Energies, 13(11): 2756. https://doi.org/10.3390/en13112756
[24] Desvita, H., Faisal, M. (2021). Characteristic of liquid smoke produced from slow pyrolysis of cacao pod shells (Theobroma cacao L). GEOMATE Journal, 20(80): 17-22. https://doi.org/10.21660/2021.80.6154
[25] Zhang, X., Yang, X., Yuan, X., Tian, S., Wang, X., Zhang, H., Han, L. (2022). Effect of pyrolysis temperature on composition, carbon fraction and abiotic stability of straw biochars: Correlation and quantitative analysis. Carbon Research, 1(1): 17. https://doi.org/10.1007/s44246-022-00017-1
[26] Li, C., Hayashi, J.I., Sun, Y., Zhang, L., Zhang, S., Wang, S., Hu, X. (2021). Impact of heating rates on the evolution of function groups of the biochar from lignin pyrolysis. Journal of Analytical and Applied Pyrolysis, 155: 105031. https://doi.org/10.1016/j.jaap.2021.105031
[27] Rodrigues, V.H., de Melo, M.M., Tenberg, V., Carreira, R., Portugal, I., Silva, C.M. (2021). Similarity analysis of essential oils and oleoresins of Eucalyptus globulus leaves produced by distinct methods, solvents and operating conditions. Industrial Crops and Products, 164: 113339. https://doi.org/10.1016/j.indcrop.2021.113339
[28] Stjepanović, M., Velić, N., Habuda-Stanić, M. (2022). Modified hazelnut shells as a novel adsorbent for the removal of nitrate from wastewater. Water, 14(5): 816. https://doi.org/10.3390/w14050816
[29] Muniyappan, G., Adenam, N.M., Muhamad Yuzaini Azrai, M.Y., Nurul Hijanah, M.H., Kernain, D., Adli, H.K. (2022). Phytochemical screening of Muntingia Calabura fruit for antioxidant and cytotoxic activities. Journal of Advanced Research in Applied Sciences and Engineering Technology, 28(1): 116-125. https://doi.org/10.37934/araset.28.1.116125
[30] Vijaya, B., Usha Rani, M. (2025). Effect of NiO nanofiller on P (VdC-Co-AN) with PEG polymer blend electrolyte for energy storage applications. Journal of Polymer Science, 63(6): 1466-1480. https://doi.org/10.1002/pol.20241029
[31] Doszhanov, Y., Atamanov, M., Jandosov, J., Saurykova, K., Bassygarayev, Z., Orazbayev, A., Sabitov, A. (2024). Preparation of granular organic iodine and selenium complex fertilizer based on biochar for biofortification of parsley. Scientifica, 2024(1): 6601899. https://doi.org/10.1155/2024/6601899
[32] Schott, J.A., Do-Thanh, C.L., Shan, W., Puskar, N.G., Dai, S., Mahurin, S.M. (2021). FTIR investigation of the interfacial properties and mechanisms of CO_2 sorption in porous ionic liquids. Green Chemical Engineering, 2(4): 392-401. https://doi.org/10.1016/j.gce.2021.09.003
[33] Izevbekhai, O.U., Gitari, W.M., Tavengwa, N.T., Ayinde, W.B., Mudzielwana, R. (2020). Response surface optimization of oil removal using synthesized polypyrrole-silica polymer composite. Molecules, 25(20): 4628. https://doi.org/10.3390/molecules25204628
[34] Jarkoni, M.N.K., Ramli, M.A.D., Wan, W.N. (2024). Effects of High-Density Polyethylene (HDPE) and additives fuel blends on diesel engine's performance and emissions and NOx prediction using boosted tree model. Journal of Advanced Research in Applied Sciences and Engineering Technology, 54(2): 269-286. https://doi.org/10.37934/araset.54.2.269286
[35] Thummajitsakul, S., Silprasit, K. (2023). Kinetics of tyrosinase inhibition, antioxidant activity, total flavonoid content and analysis of *Averrhoa bilimbi* L. Extracts and its fruit vinegar using FTIR and multivariate methods. Trends in Sciences, 20(2): 3641-3641. https://doi.org/10.48048/tis.2023.3641
[36] Martínez-Toledo, C., Valdes-Vidal, G., Calabi-Floody, A., González, M.E., Ruiz, A., Mignolet-Garrido, C., Norambuena-Contreras, J. (2025). Optimising slow pyrolysis parameters to enhance biochar European hazelnut shell as a biobased asphalt modifier. Materials Today Sustainability, 30: 101087. https://doi.org/10.1016/j.mtsust.2025.101087
[37] Wang, W., Bai, J., Lu, Q., Zhang, G., Wang, D., Jia, J., Yu, L. (2021). Pyrolysis temperature and feedstock alter the functional groups and carbon sequestration potential of Phragmites australis-and Spartina alterniflora-derived biochars. GCB Bioenergy, 13(3): 493-506. https://doi.org/10.1111/gcbb.12795
[38] Gezahegn, S., Sain, M., Thomas, S.C. (2019). Variation in feedstock wood chemistry strongly influences biochar

liming potential. Soil Systems, 3(2): 26. https://doi.org/10.3390/soilsystems3020026
[39] Saputra, I., Prijono, S., Suntari, R. (2024). Optimization of biochar quality from palm and cacao waste through variation of pyrolysis temperature and duration as a soil amendment material. OnLine Journal of Biological Sciences, 24(4): 765-776. https://doi.org/10.3844/ojbsci.2024.765.776
[40] Ngatia, L.W., Hsieh, Y.P., Nemours, D., Fu, R., Taylor, R.W. (2017). Potential phosphorus eutrophication mitigation strategy: Biochar carbon composition, thermal stability and pH influence phosphorus sorption. Chemosphere, 180: 201-211. https://doi.org/10.1016/j.chemosphere.2017.04.012
[41] Ippolito, J. A., Cui, L., Kammann, C., Wrage-Mönnig, N., Estavillo, J.M., Fuertes-Mendizabal, T., Borchard, N. (2020). Feedstock choice, pyrolysis temperature and type influence biochar characteristics: A comprehensive meta-data analysis review. Biochar, 2(4): 421-438. https://doi.org/10.1007/s42773-020-00067-x
[42] Naghipour, D., Amouei, A., Taher Ghasemi, K., Taghavi, K. (2019). Removal of metoprolol from aqueous solutions by the activated carbon prepared from pine cones. Environmental Health Engineering and Management Journal, 6(2): 81-88. https://doi.org/10.15171/ehem.2019.09
[43] Wang, H., Zhang, M., Lv, Q. (2019). Influence of pyrolysis temperature on cadmium removal capacity and mechanism by maize straw and platanus leaves biochars. International Journal of Environmental Research and Public Health, 16(5): 845. https://doi.org/10.3390/ijerph16050845
[44] Roshan, A., Ghosh, D., Maiti, S.K. (2023). How temperature affects biochar properties for application in coal mine spoils? A meta-analysis. Carbon Research, 2(1): 3. https://doi.org/10.1007/s44246-022-00033-1
[45] Chatterjee, R., Sajjadi, B., Chen, W.Y., Mattern, D.L., Hammer, N., Raman, V., Dorris, A. (2020). Effect of pyrolysis temperature on physicochemical properties and acoustic-based amination of biochar for efficient CO_2 adsorption. Frontiers in Energy Research, 8: 85. https://doi.org/10.3389/fenrg.2020.00085
[46] Raaen, S. (2021). Adsorption of carbon dioxide on mono-layer thick oxidized samarium films on Ni (100). Nanomaterials, 11(8): 2064. https://doi.org/10.3390/nano11082064
[47] Mazurek, K., Drużyński, S., Kiełkowska, U., Szłyk, E. (2021). New separation material obtained from waste rapeseed cake for copper (II) and zinc (II) removal from the industrial wastewater. Materials, 14(10): 2566. https://doi.org/10.3390/ma14102566
[48] Zhang, G., Liu, N., Luo, Y., Zhang, H., Su, L., Oh, K., Cheng, H. (2020). Efficient removal of Cu (II), Zn (II), and Cd (II) from aqueous solutions by a mineral-rich biochar derived from a spent mushroom (Agaricus bisporus) substrate. Materials, 14(1): 35. https://doi.org/10.3390/ma14010035
[49] Brunauer, S., Emmett, P.H., Teller, E. (1938). Adsorption of gases in multimolecular layers. Journal of the American Chemical Society, 60(2): 309-319. https://doi.org/10.1021/ja01269a023
[50] Zelenka, T., Horikawa, T., Do, D.D. (2023). Artifacts and misinterpretations in gas physisorption measurements and characterization of porous solids. Advances in Colloid and Interface Science, 311: 102831. https://doi.org/10.1016/j.cis.2022.102831
[51] Zhou, X., Li, Y., Hart, K.E., Abbott, L.J., Lin, Z., Svec, F., Turner, S.R. (2013). Nanoporous structure of semirigid alternating copolymers via nitrogen sorption and molecular simulation. Macromolecules, 46(15): 5968-5973. https://doi.org/10.1021/ma4006582
[52] Ambroz, F., Macdonald, T.J., Martis, V., Parkin, I.P. (2018). Evaluation of the BET Theory for the Characterization of Meso and Microporous MOFs. Small Methods, 2(11): 1800173. https://doi.org/10.1002/smtd.201800173
[53] Singh, L., Kaur, L., Singh, G., Dhawan, R.K., Kaur, M., Kaur, N., Singh, P. (2022). Determination of alteration in micromeritic properties of a solid dispersion: Brunauer-Emmett-Teller based adsorption and other structured approaches. AAPS PharmSciTech, 23(6): 209. https://doi.org/10.1208/s12249-022-02367-w
[54] Desmurs, L., Galarneau, A., Cammarano, C., Hulea, V., Vaulot, C., Nouali, H., Sachse, A. (2022). Determination of microporous and mesoporous surface areas and volumes of mesoporous zeolites by corrected t-plot analysis. ChemNanoMat, 8(4): e202200051. https://doi.org/10.1002/cnma.202200051
[55] Kwiatkowski, M., Kalderis, D. (2020). A complementary analysis of the porous structure of biochars obtained from biomass. Carbon Letters, 30(3): 325-329. https://doi.org/10.1007/s42823-019-00101-4